5

Major Tsunami Risks from Splay Faulting

Mohammad Heidarzadeh
Assistant professor, Department of Civil Engineering, Tarbiat Modares University
Tehran,
Iran

1. Introduction

One of the main lessons learned from the great 2004 Sumatra-Andaman earthquake was the fact that tsunami generation process due to large subduction earthquakes is rather complicated. Hence, modelling tsunamis by assuming a simple rupture on a megathrust may not account for actual variations of observed tsunami runups in the near field. From this viewpoint, the 2004 Indian Ocean tsunami was a milestone in tsunami research in that it clearly showed the effect of secondary tsunami sources on intensifying the near-field tsunami heights. The phenomena that are triggered by the main subduction earthquakes and locally contribute to tsunami in addition to the main slip on the subduction zone are known as secondary tsunami sources. The most important secondary sources are submarine landslides, whose effect was mainly evidenced during the 1992 Flores Island tsunami (Synolakis and Okal, 2005; Hidayat et al., 1995), and splay fault branching which was observed during some large subduction earthquakes such as the 1946 Nankai tsunami (Cummins and Kaneda, 2000), 1960 Chilean and 1964 Alaskan tsunamis (Plafker, 1972), and most recently during the 2004 Sumatra-Andaman earthquake and tsunami (Sibuet et al., 2007).

Here, in this chapter we focus on splay faults which are known as one of the important secondary tsunami sources and were responsible for a large part of tsunami deaths during past tsunamis. Splay faults, sometimes known as imbricate faults, are steeply-dipping thrust faults which branch upward from the subduction zone to the seafloor. As splay faults often have steep dip angles, they are capable of producing large seafloor deformation which can significantly increase tsunami runup heights in the near-field. Figure 1 schematically shows a splay fault which branches from the plate boundary. As shown, an abrupt increase in seafloor uplift happens at the location of the splay fault. It is clear that this enhanced seafloor uplift will cause larger tsunami wave heights in the near field.

With this background, it is clear that tsunami hazard assessment without taking into account the effect of possible splay fault branching due to large subduction zone earthquakes may result in underestimating the actual existing tsunami hazards. Hence, in this chapter we study the consequences of splay faulting on tsunami waves in the near-field. First, we make a review of some actual splay faulting cases. Then, the characteristics of splay fault branching from the main plate boundary will be discussed. In the next section, numerical modeling of tsunami will be performed to investigate the effect of splay faulting on tsunami wave heights in the near-field. Finally, we make some practical

recommendations on how to take into account the effect of splay faulting for tsunami hazard assessment.

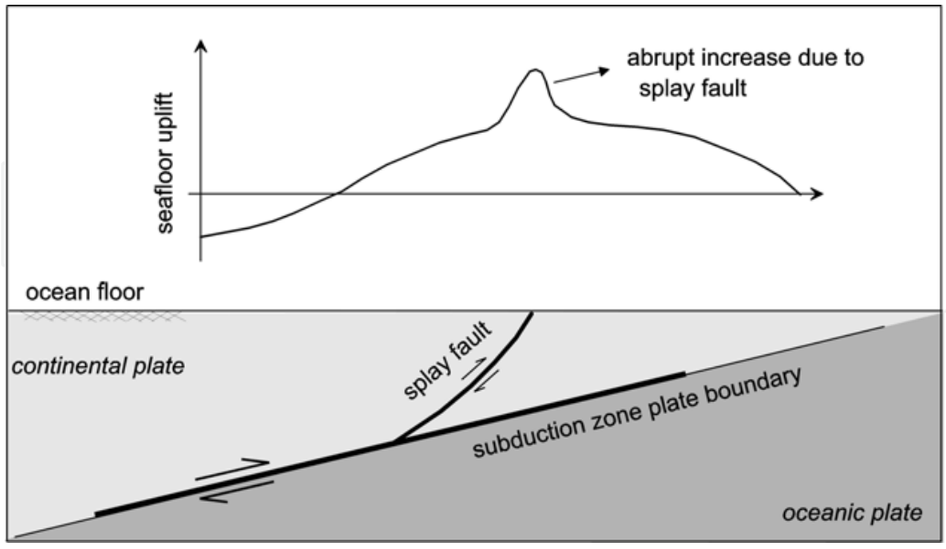

Fig. 1. Sketch showing a splay fault branching upward from a subduction zone plate boundary (bottom) along with the variation of seafloor uplift due to the earthquake (top).

2. Characteristics of splay fault branching

Although we do not intend in this chapter to study the dynamics of splay fault branching from geological and seismological point of views, but basic information on splay faulting can be useful in view of tsunami hazard assessment.

Many studies show that splay faults exist in most subduction zones in the world (Sykes and Menke, 2006; Ryan and Scholl, 1989). According to Sykes and Menke (2006), splay faults are common in most modern accretionary prisms, which grow as sediments are added from the upper plate. These thrust faults in accretionary prisms may rupture due to great subduction zone earthquakes. Fukao (1979) suggested that rupture propagation onto splay faults within accretionary wedges is one of the main mechanisms for generating large tsunamis. According to Park et al. (2002), as splay faults are relatively weak zones within accretionary prisms, it is likely that these weak zone to be repeatedly selected for rupture propagation of subduction earthquakes.

In fact, different studies showed that the total slip during a large megathrust earthquake can be partitioned between the subduction-zone plate boundary and splay faults within the accretionary wedge (e.g., Baba et al., 2006). The amount of slip that transfers from the plate boundary onto splay faults during large subduction earthquakes and the pattern of slip partitioning between them can be an important issue in view of tsunami hazard assessment because the vertical seafloor uplift due to splay faults is relatively larger resulting in large tsunamis. However, the pattern of slip partitioning between subduction zone and splay faults seems casual (Park et al., 2002; Baba et al., 2006). In addition, it is not known if splay faults can rupture occasionally by themselves or not (Sykes and Menke, 2006).

Despite this, some authors made efforts to study the complex phenomenon of splay fault branching during large subduction earthquakes. Cooke (1997) studied the effect of frictional

strength variations near fault tips on the pattern of splay fault branching. The result of his work is shown in Fig. 2 indicating that gradual changes in frictional strength may produce broad zones of splay fractures, whereas abrupt changes in frictional strength produce single splay fractures. Kame et al. (2003) studied the effects of pre-stress state, rupture velocity, and branch angle on dynamic fault branching. Their study showed that the pre-stress state has a significant effect on the most favored direction for dynamic branching. Kame et al. (2003) showed that the enhanced dynamic stressing of a rapidly propagating rupture could nucleate failure on a fault which would not necessarily be judged the most favorably oriented one based on the pre-stress state. In summary, Kame et al. 's (2003) study revealed that the tendency of a fault to branch depends on the orientation of the local pre-stress field relative to that of the main fault, the rupture velocity, and the angle between the main and the branching faults.

Fliss et al. (2005) studied the relationship between fault branching and rupture directivity. Wang and Hu (2006) presented a new theory to explain accretionary prisms in subduction earthquake cycles. This theory provides a conceptual framework for investigating the evolution history of accretionary prisms and forearc basins and related phenomena like splay-faulting during great earthquakes and its role in accommodating deformation and generating tsunami.

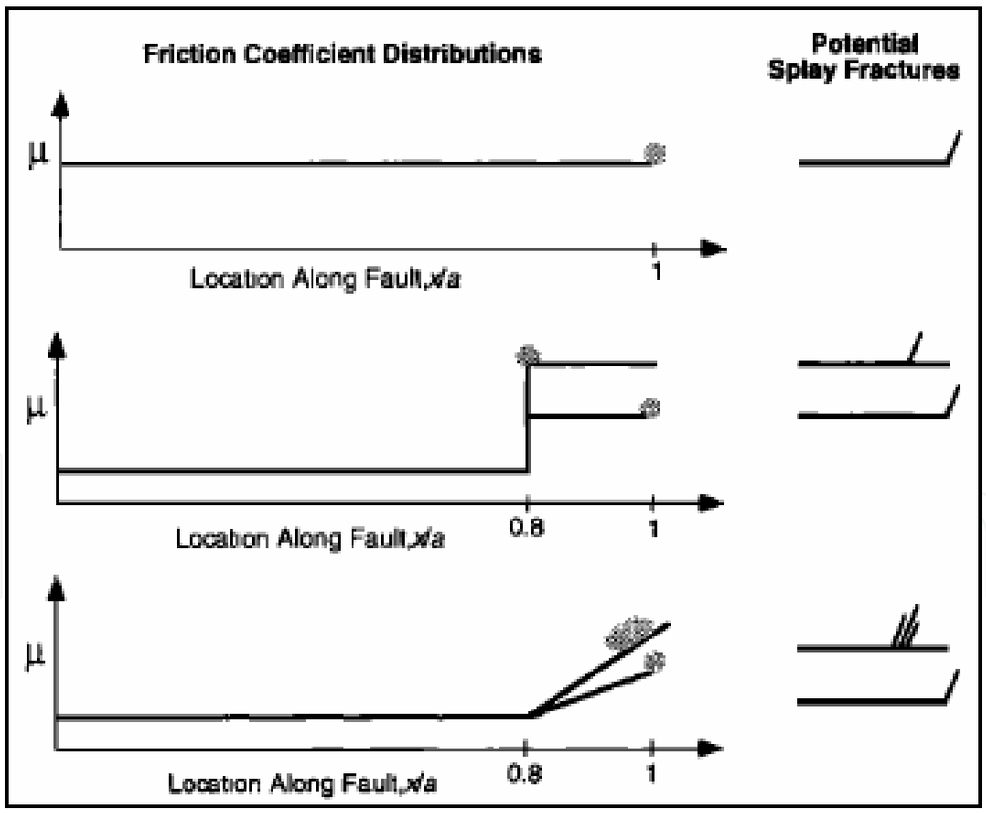

Fig. 2. The effect of frictional strength variations near fault tips on the pattern of splay fault branching. Uniform friction coefficient produces single fractures (top and middle graphs). Linear increases in friction coefficient can produce broad zones of splay fractures near the fault tip (bottom graph). Region of potential splay cracks is shaded (After Cooke, 1997).

Others who studied the mechanism of splay fault branching are: Bhat et al. (2007), Schulson et al. (1999), and Paliakov et al. (2002).

3. Review of some splay faulting cases

The pronounced effect of splay faulting on tsunami wave heights in the near-field was evidenced during some large tsunamis like 1946 Nankai earthquake and tsunami, 1960 Chilean and 1964 Alaskan earthquakes and tsunamis, and most recently during the 2004 great Sumatra-Andaman earthquake and tsunami.

The seafloor deformation caused by the 1964 Alaskan earthquake along with the tectonic setting of the Aleutian subduction zone is shown in Fig. 3. As can be seen, the 1964 Alaskan earthquake with a moment magnitude of *Mw* 9.2 (Kanamori, 1977), was associated with a major splay faulting at the location of the Fatton Bay Fault which locally increased the seafloor uplift by a factor of 2. The seafloor uplift was around 12 m at the location of the splay fault branching (Fig. 3-top) whereas its maximum value was around 6 m at the adjacent regions. It is clear that such a large seafloor deformation can cause a catastrophic tsunami because the maximum near-filed tsunami runup is a direct function of the seafloor deformation at the earthquake source (Synolakis, 2003). In other words, the larger the vertical seafloor deformation in the earthquake source, the larger the tsunami runup heights that is produced.

The other well-known case of splay fault branching during a large subduction earthquake is the 1960 Chilean earthquake and tsunami which is the largest ever recorded earthquake with a moment magnitude of *Mw* 9.5 (Kanamori, 1977). The rupture mechanism of this earthquake was thoroughly studied by Plafker (1972). A summary of the seafloor vertical uplift caused by the earthquake and the tectonic setting of the Peru-Chile subduction zone is shown in Fig. 4. It is clear in Fig. 4 that the seafloor uplift is significantly larger in the vicinity of the splay fault compared to that of the adjacent regions.

Other cases of splay fault branching are the 1946 Nankai (*Mw* 8.3) and 1944 Tonankai (*Mw* 8.1) earthquakes both originated at the Nankai subduction zone, southwest Japan. Studies show that perhaps the Nankai subduction zone is susceptible to splay fault branching and many splay faults exist in this subduction zone (Cummins and Kaneda, 2000 ; Sunagawa and Hayashi, 2007; Cummins et al., 2001). The presence of splay faults at the location of Nankai subduction zone was studied by Park et al. (2002) using seismic reflection data (Fig. 5). The location of splay faults are shown in Fig. 5 by green arrows.

We may point out the great 2004 Sumatra-Andaman earthquake and tsunami as another example. Plafker et al. (2007) and Sibuet et al., (2007) presented evidence that the 2004 Indian Ocean tsunami was associated with a splay fault originating at the interplate fault plane which increased the tsunamigenic effects.

4. Modelling the effect of splay fault branching on tsunami waves

In this section, the effect of splay faulting in a subduction zone on tsunami waves will be studied using numerical modelling of tsunami waves. As a case study, the Makran subduction zone (MSZ) at the north-western Indian Ocean will be considered for our modelling efforts.

As shown in Fig. 6, the MSZ is formed by the northward subduction of the Arabian plate beneath the Eurasian one. This zone extends east from the Strait of Hormoz in Iran to near

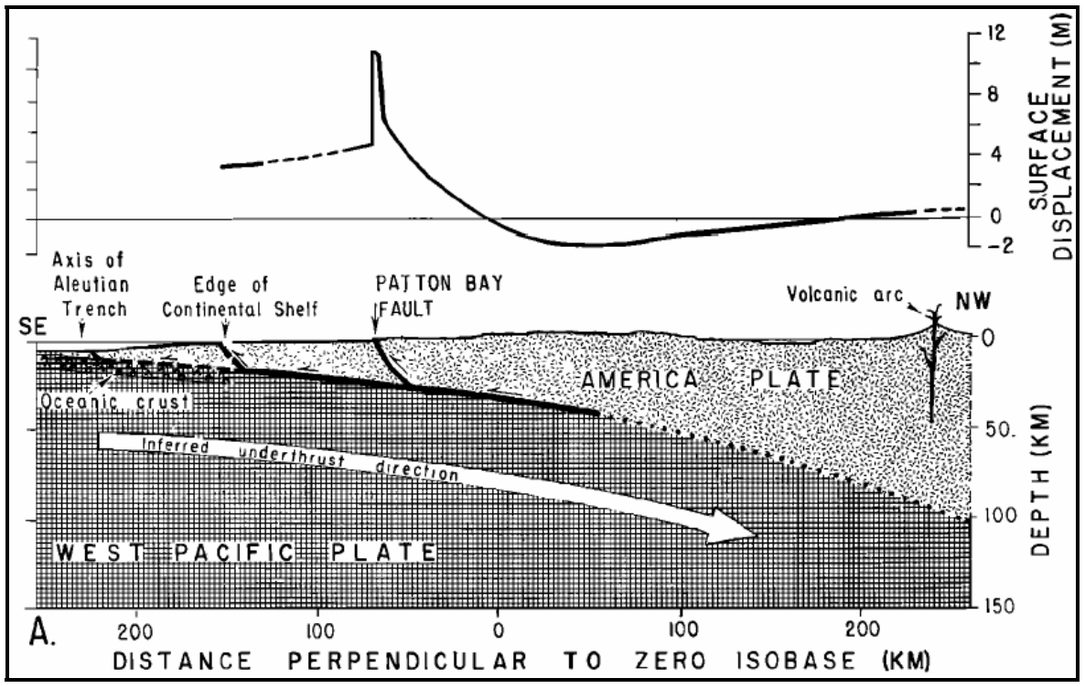

Fig. 3. Seafloor deformation caused by the 1964 Alaskan earthquake (top), and branching of a splay fault at the Patton Bay Fault location (bottom). (After Plafker, 1972).

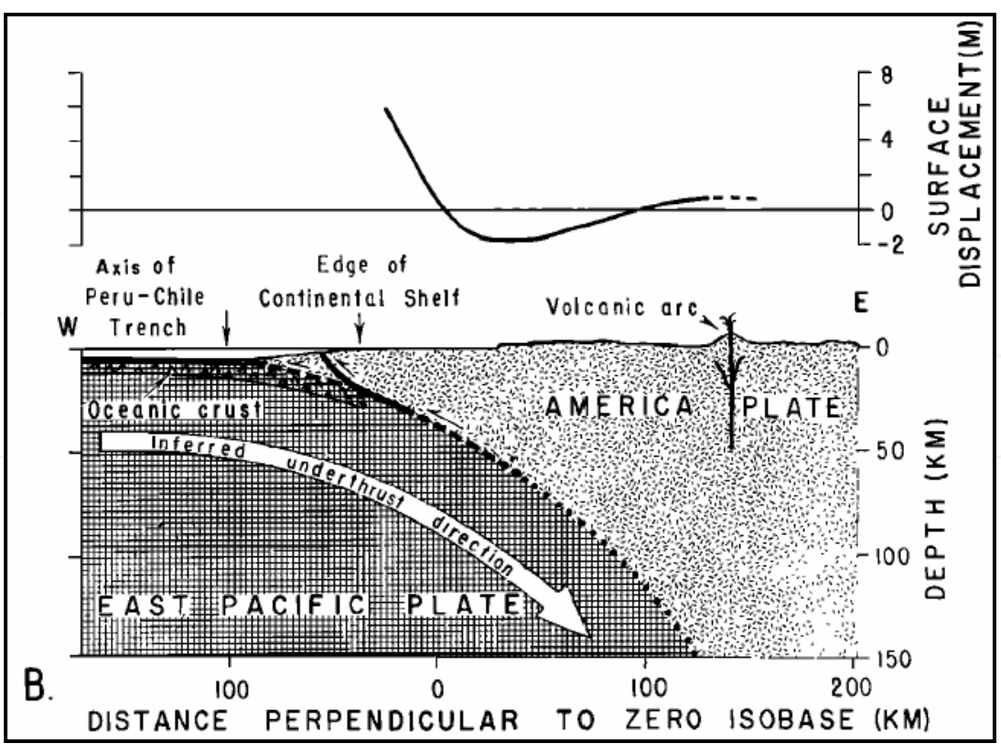

Fig. 4. Seafloor deformation caused by the 1960 Chilean earthquake (top), and branching of a splay fault (bottom). (After Plafker, 1972).

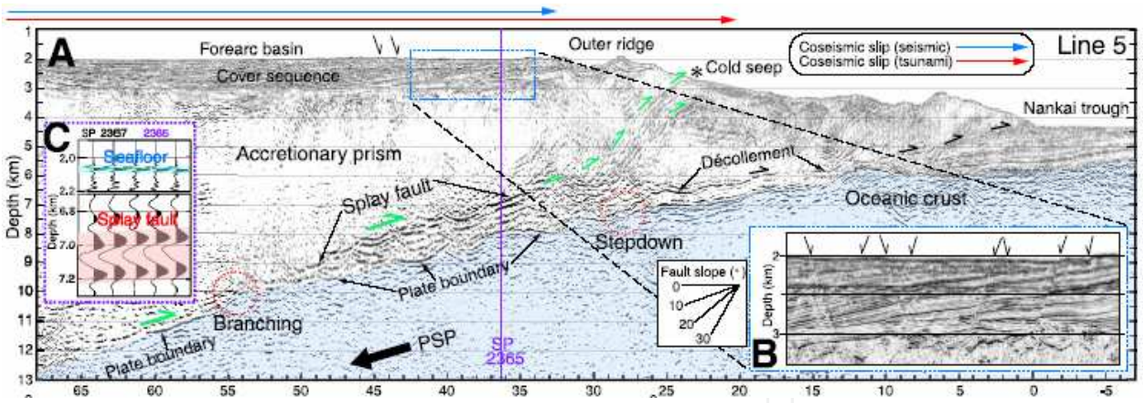

Fig. 5. Multichannel seismic profiles obtained at the location of Nankai subduction zone showing the splay faults (A). Green and black arrows show motions of the splay fault slip and the décollement or normal fault, respectively. Locations of both the splay fault's initial branching and the décollement stepdown to the top of the oceanic basement are marked in red dotted circles. Note active normal faults (inset B) cutting the well-stratified, landward tilting cover sequence and reverse polarity reflection (inset C) of the splay fault at ~7km depth around shot point (SP) 2365. (After Park et al., 2002).

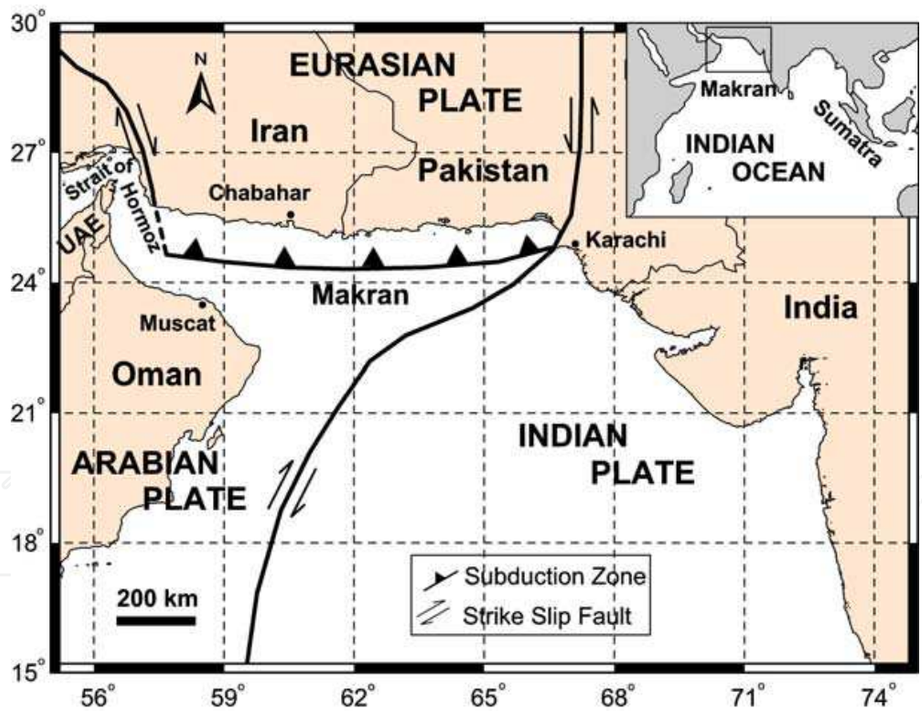

Fig. 6. General map of the Makran subduction zone and its tectonic setting.

Karachi in Pakistan with a length of about 900 km. The reasons that we have chosen the MSZ for our case study are twofold: firstly, Heidarzadeh et al. (2008) presented evidence that a splay fault may have been responsible for the huge runup heights observed in the near field during the Makran earthquake and tsunami of November 27, 1945, and secondly, Mokhtari et al. (2008) showed that many splay faults are present in the MSZ using 2D

seismic reflection profiles. Figure 7 is an example of the 2D seismic reflection profiles presented by Mokhtari et al. (2008). In addition, the Makran region has one of the largest accretionary wedges on the earth with an extreme sediment thickness of about 7 km indicating a high probability for splay fault branching due to large subduction earthquakes. Therefore, it can be seen that splay fault branching is a matter of concern in the MSZ and it is likely that this phenomenon occur during large subduction earthquakes in this region. As a result, the possible effect of splay fault branching on tsunami waves should be taken into account for any tsunami hazard assessment in this region.
Here, to quantitatively evaluate the effect of splay faulting on tsunami waves, we numerically model a large earthquake and the consequent tsunami in the MSZ twice: with and without considering a splay fault branching. In the following subsections, the details of our modellings will be presented.

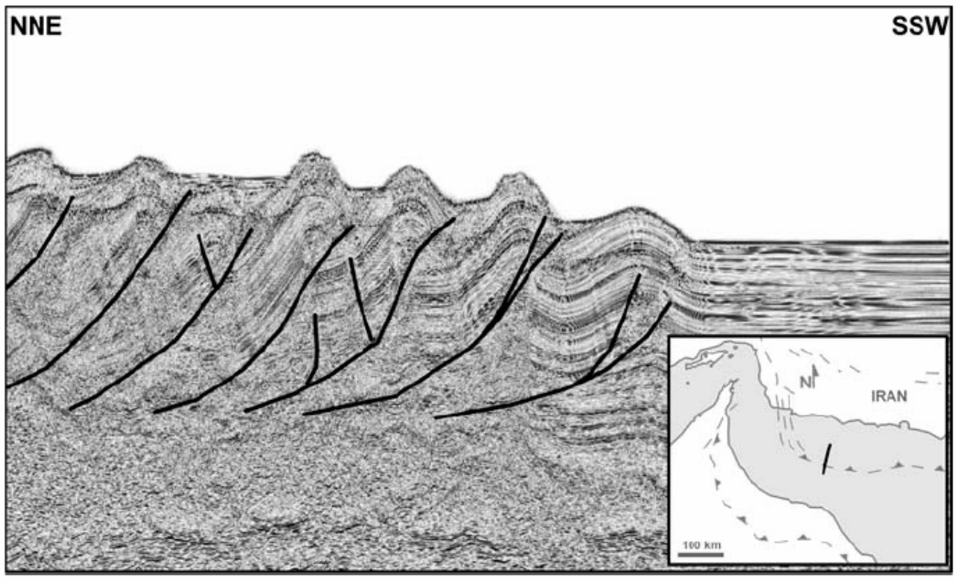

Fig. 7. An example of 2D seismic reflection profiles obtained at the Makran subduction zone (MSZ). The thick lines show the locations of splay faults. The inset at the bottom-right shows the location of the profile in the MSZ (After Mokhtari et al., 2008).

4.1 The earthquake scenario and tsunami source modelling

To realistically choose the scenario earthquake for our tsunami simulations, we first review the history of large earthquake occurrence in the MSZ. This will help understand which parts of the MSZ are susceptible to fail into large-size earthquakes.
Historical earthquakes in the MSZ were studied by some authors including Quittmeyer and Jacob (1979), Page et al. (1979), Ambraseys and Melville (1982), and Byrne et al. (1992). A review of these studies indicates that the Makran region experienced at least seven large earthquakes (M>7) in the past 500 years rupturing the plate boundary in four different segments as shown in Fig. 8. Also, the information of these large earthquakes is summarized in Table 1. As indicated in Fig. 8 by a question mark, the event of 1483 in the western Makran is uncertain, and some authors believe that the western Makran is entirely aseismic.
As the earthquake scenario in this study, we suppose that the blocks A, B, and C shown in Fig. 8 are ruptured simultaneously. This scenario was previously used by Okal and

Synolakis (2008). The reason behind this is the study by Stein and Okal (2007) who proposed that the maximum earthquake size expected from a subduction zone depends on the length of a continuous fault system along a convergent plate boundary. This continuous segment is about 500 km (blocks A, B, and C in Fig. 8) for the MSZ as the segmentation of this subduction zone was confirmed by Byrne et al. (1992).

The tsunami modeling process can be divided into three parts: generation, propagation, and runup (Synolakis, 2003). Generation modeling forms the first stage in the modeling of tsunami, and includes the calculation of the initial disturbance of ocean surface due to the earthquake–triggered deformation of the seafloor using seismic parameters.

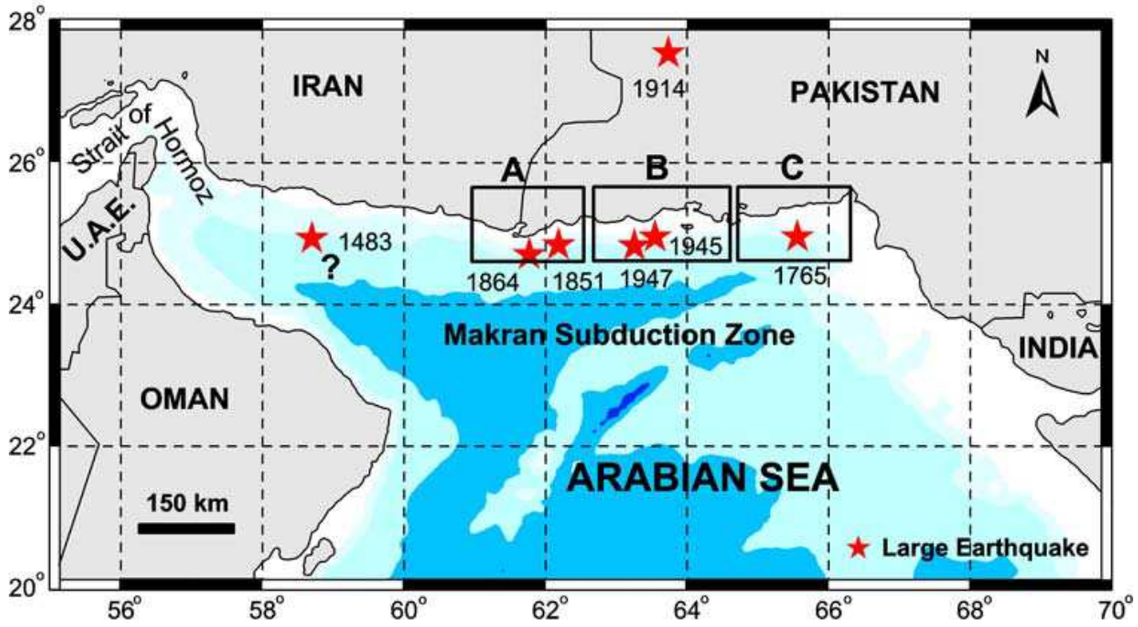

Fig. 8. Large historical earthquakes in the Makran subduction zone (stars) showing the different segments of the plate boundary which ruptured due to large earthquakes (modified from Byrne et al., 1992 and Okal and Synolakis, 2008).

No.	Date (yyyy-mm-dd)	Latitude (°N)	Longitude (°E)	Ms	Mw	Intensity (MM)	Focal depth (km)
1	1483-??-??	24.90	57.90			10	
2	1765-??-??	25.40	65.80			8–9	
3	1851-04-19	25.10	62.30			8–9	
4	1864-??-??	25.12	62.33			6–8	
5	1914-??-??	29.70	63.80	7.0			
6	1945-11-27	24.50	63.00		8.1		25.0
7	1947-08-05	25.10	63.40		7.6		35.0

Table 1. Summary of the information of the past large earthquakes in the MSZ.
Abbreviations are: MM, Modified Mercalli; Ms, Surface wave magnitude; Mw, earthquake moment magnitude; °N, degree North; and °E, degree East.

The algorithm of Mansinha and Smylie (1971) was used to calculate the seafloor deformation. This algorithm is based on seismic parameters that include the strike, dip, and slip angles, the amount of slip, the dimensions of the ruptured area (length and width), and the earthquake depth. Empirical equations of Wells and Coppersmith (1994) were used to estimate the corresponding earthquake magnitude of the fault rupture followed by calculation of the rupture width and surface displacement. We validated the predictions of the empirical equations using the available seismic parameters of the 1945 event. The only instrumentally recorded large earthquake at Makran is the event of 1945 (Mw 8.1) rupturing approximately one–fifth of the plate boundary and causing about 7 m of slip (Byrne et al., 1992). Table 2 (first row) presents the source parameters for the scenario earthquake that we evaluate in this study. As shown in Table 2, the scenario earthquake features a seismic moment of about 1.95×10^{22} N m (1.95×10^{29} dyne × cm).

For the case that the earthquake is associated with splay fault branching, a hypothetical splay fault inspired by the 1946 Nankai and 1960 Chilean earthquakes was assumed to branch during the scenario earthquake. Table 2 (rows 2 and 3) presents the seismic parameters of the splay fault and the main plate boundary slips for this new earthquake. We note that the seismic moment of this earthquake was kept unchanged and was the same as that of the first scenario (Table 2- last column). Therefore, due to the slip on the splay fault, the maximum slip on the main plate boundary was reduced.

Using the seismic parameters presented in Table 2 for the two cases of with and without splay fault branching, tsunami source modelling is performed whose results are shown in Fig. 9. The maximum seafloor uplift due to the scenario earthquake was about 4.5 m without splay fault branching (solid line– Fig. 9-top) which was raised to 7.2 m due to the presence of the splay fault. However, it should be noted that Fig. 9 shows that the increase in the amount of the seafloor uplift is limited to the areas close to the splay fault.

Case	Mw	Slip type	L	W	D	H	δ	λ	φ	Earthquake moment (N.m) ┼
Without SF	8.6	PB slip	500	100	13	25	7	90	265	1.95×10^{22}
With SF	8.6	PB slip	500	100	12	25	7	90	265	1.95×10^{22}
		SF slip	100	50	10	15	30	90	265	

Table 2. Source parameters of the scenario earthquake with and without splay faulting in the MSZ. Abbreviations are: SF, Splay Fault; Mw, earthquake moment magnitude; PB, Plate Boundary; L, rupture Length in km; W, rupture Width in km; D, fault Displacement in m; H, earthquake depth in km; δ, dip angle in degrees; λ, slip angle in degrees; and φ, strike angle in degrees. The rigidity of the earth is considered to be 3×10^{10} N m^{-2}.

4.2 Tsunami modelling

The numerical model TUNAMI–N2 was used for modelling tsunami propagation and coastal amplifications. The model was developed by Nobuo Shuto and Fumihiko Imamura of the Disaster Control Research Center in Tohoku University (Japan) through the Tsunami Inundation Modeling Exchange (TIME) program (Goto et al., 1997). TUNAMI–N2 is one of the key tools for numerical modeling of wave propagation and coastal amplification of

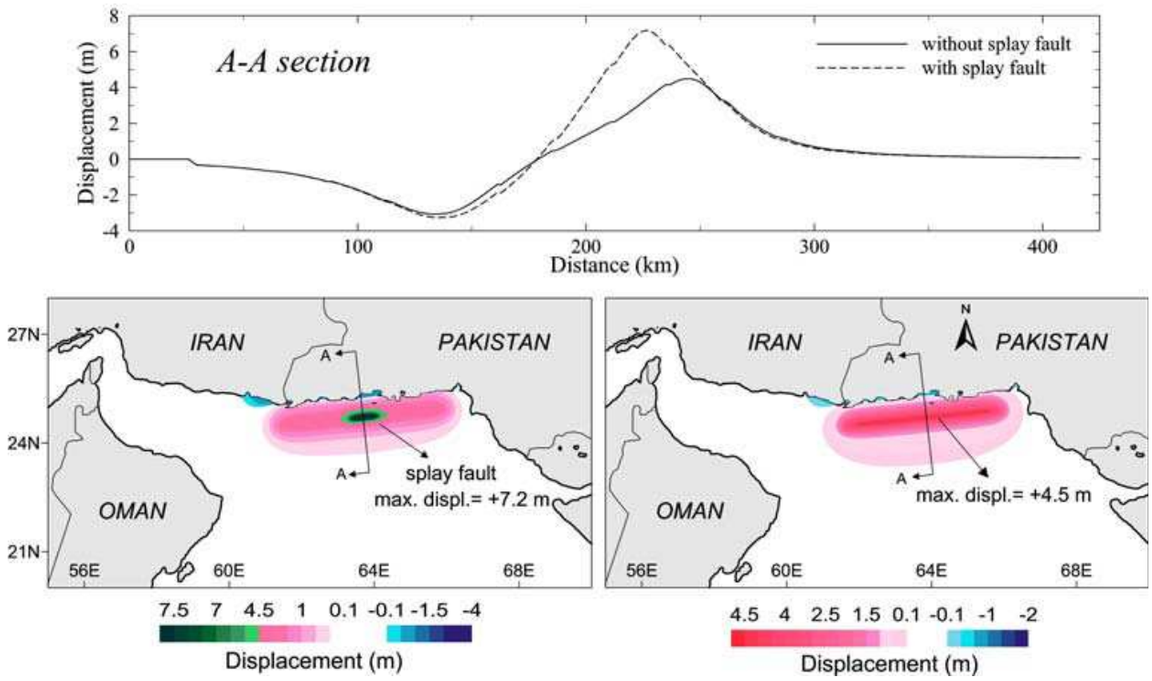

Fig. 9. Results of tsunami source modelling for the cases of without (right panel) and with (left panel) splay fault branching.

tsunami in relation to different initial conditions (Yalciner et al., 2004). A similar methodology is used in the numerical model MOST (Method Of Splitting Tsunami) developed by Titov and Synolakis (1997). TUNAMI–N2 and MOST are nonlinear shallow water codes that have yielded satisfactory agreement with laboratory and field data (Yeh et al., 1996).

We used a 833 × 444 grid and 369852 grid points in our computational domain. The time step was 1.0 s to satisfy the stability condition. The duration of tsunami propagation was 3 h. Bathymetry data provided through the GEBCO digital atlas (General Bathymetric Chart of the Oceans) was applied in this study (IOC et al., 2003). As runup modeling is not applicable to large computational domains, we calculated the maximum positive tsunami heights along the coast which give a reasonable approximation of the runup heights (Tinti et al., 2006).

Snapshots of tsunami propagation for both cases are shown in Fig. 10 at different times of 10, 30, and 60 minutes after the earthquake. Also, to evaluate the effect of splay faulting on tsunami wave heights, the distribution of tsunami wave heights along the north coast of the MSZ (i.e., the southern coast of Iran and Pakistan) are shown in Fig. 11 for the both cases. Results of tsunami modeling (Fig. 11) reveal that possible splay faulting during large mega–thrust earthquakes in the MSZ can locally increase the maximum tsunami wave height by nearly a factor of 2. Based on Fig. 11, the maximum simulated wave height is about 12 m in the vicinity of the splay fault while it was about 6 m at the same location in the previous simulation. Similar to the seafloor uplift pattern, the effect of splay fault branching on the distribution of tsunami wave height is localized to the vicinity of the splay fault. In other words, the effect of possible splay fault branching on tsunami is limited to the near field. As shown in Fig. 10, no significant difference can be observed in tsunami snapshots for the two cases of with and without splay faulting in the far field.

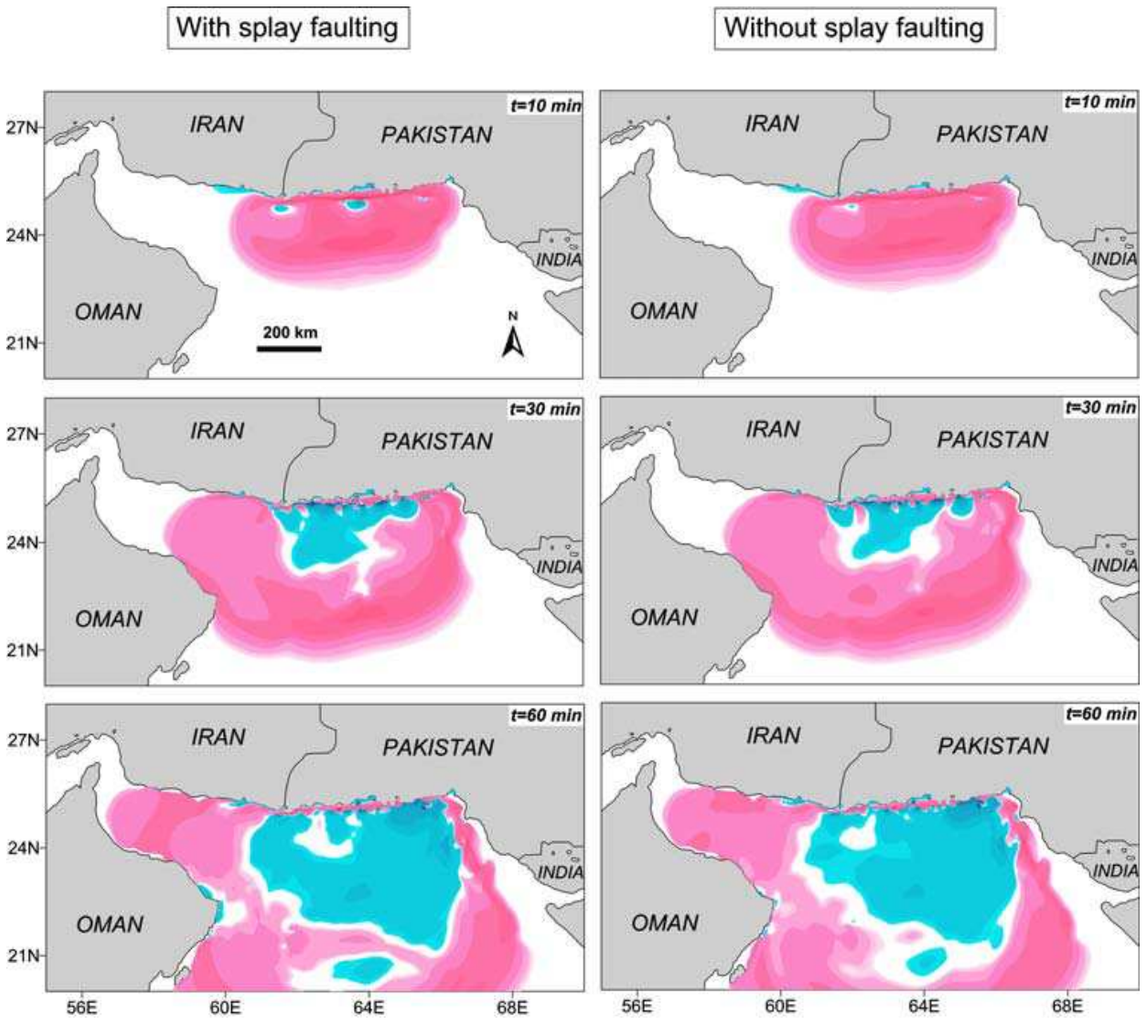

Fig. 10. Snapshots of tsunami simulations due to the two cases of without (right columns) and with (left columns) splay fault branching at different times.

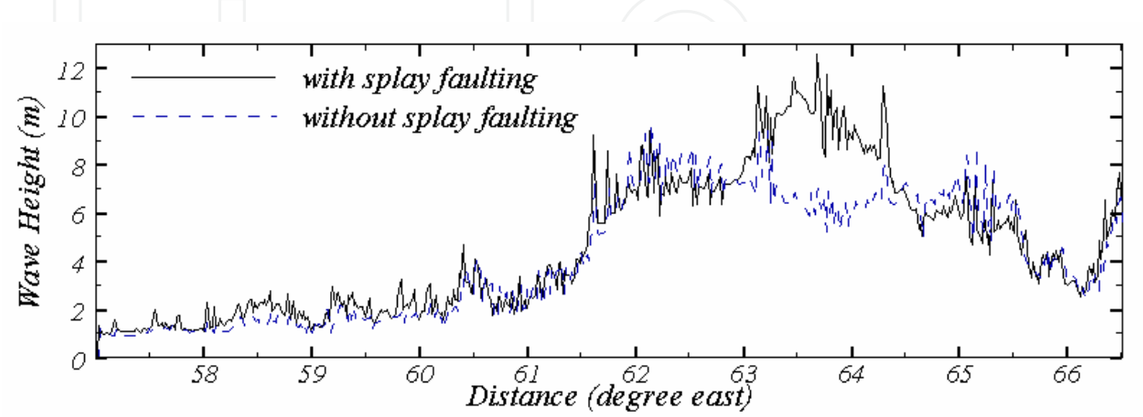

Fig. 11. Distribution of tsunami wave heights along the north coast of the MSZ (i.e., the southern coasts of Iran and Pakistan) due to the two cases of with and without tsunami.

The above results are consistent with the observations of tsunami runup during some actual large tsunami. For example, Plafker et al. (2007) reported that the peak runup was as high as 39 m west of Banda Aceh during the 2004 Indian Ocean tsunami while they were about 5 to 12 m along the north coast and 7 to 20 m along the west coast of Indonesia. Plafker et al. (2007) attributed the huge runup height observed in west of Banda Aceh to splay faulting.

5. Indications for tsunami hazard assessment and recommendations

We showed that the branching of a hypothetical splay fault from the plate boundary during large subduction earthquakes can locally increase the maximum wave height by nearly a factor of 2. In our modeling, a slip of 10 m was supposed on the splay fault. It is evident that the larger the slip on the splay fault, the larger the runup height that is produced. The increase of local runup by a factor of about 2 or more due to a splay fault branching was previously documented by field surveys, e.g., the 2004 Indian Ocean tsunami (Plafker et al., 2007), the 1960 Chilean and 1964 Alaskan tsunami (Plafker, 1972). Therefore, for planning purposes, it seems reasonable and conservative to consider that local runup may be at least twice the amount estimated from modeling studies.

As discussed by some authors previously, tsunami sources due to large subduction earthquakes can be more complicated than a simple slip on the plate boundaries as other phenomena like splay fault branching are likely to occur. Therefore, it is essential that these effects to be taken into account for tsunami modelling.

Furthermore, the pronounced effect of splay faulting on the local runup height may highlight the need for future research to investigate which parts of a particular subduction zone are more likely to experience this phenomenon during large earthquakes.

6. Conclusions

To quantitatively investigate the effect of possible splay faulting on intensifying tsunami wave heights, a large earthquake and tsunami (Mw 8.6) was numerically modelled in the Makran subduction zone for two cases of with and without splay fault branching. In this study, a hypothetical splay fault was used whose seismic parameters were inspired by the 1946 Nankai and 1960 Chilean earthquakes. Modelling of a hypothetical splay fault showed that it can locally increase the maximum wave height by nearly a factor of 2. Hence, for planning purposes, we propose a safety factor of 2 for the tsunami wave heights obtained from regular tsunami simulations.

7. References

Ambraseys, N.N., & Melville, C.P. (1982). A history of Persian earthquakes. Cambridge University Press, Cambridge, Britain, 218 pp.

Baba, T., Cummins, Ph.R., Hori, T., & Kaneda, Y. (2006). High precision slip distribution of the 1944 Tonankai earthquake inferred from tsunami waveforms: Possible slip on a splay fault, *Tectonophysics,* 426, 119–134, doi:10.1016/j.tecto.2006.02.015.

Bhat, H.S., Olives, M., Dmowska, R., & Rice, J.R. (2007). Role of fault branches in earthquake rupture dynamics, *Journal of Geophysical Research,* 112, B11309, pp. 1-16.

Byrne, D.E., Sykes, L.R., & Davis, D.M., (1992). Great thrust earthquakes and aseismic slip along the plate boundary of the Makran subduction zone. *Journal of Geophysical Research* , 97, B1, pp. 449–478.

Cooke, M.L. (1997). Fracture localization along faults with spatially varying friction. *Journal of Geophysical Research,* 102, B10, pp.22425-22434.

Cummins, Ph.R. ; & Kaneda, Y. (2000). Possible splay fault slip during the 1946 Nankai earthquake. *Geophysical Research Letters,* 27, 17, pp. 2725–2728.

Cummins, Ph.R., Hori, T., & Kaneda, Y. (2001). Splay fault and megathrust earthquake slip in the Nankai Trough, *Earth Planets Space*, 53, 243–248.

Fliss, S., Bhat, H.S., Dmowska, R., & Rice, J.R. (2005). Fault branching and rupture directivity, Journal of Geophisical Research, 110, B06312, pp. 1-22.

Fukao, Y. (1979). Tsunami earthquakes and subduction processes near deep-sea trenches. *Journal of Geophysical Research*, 84, pp. 2303–2314.

Goto, C., Ogawa, Y., Shuto, N., & Imamura, F. (1997). Numerical method of tsunami simulation with the leap–frog scheme (IUGG/IOC Time Project), IOC Manual, UNESCO, No. 35.

Kame, N., Rice, J.R., & Dmowska, R. (2003). Effects of prestress state and rupture velocity on dynamic fault branching, Journal of Geophysical Research, 108, B5, pp. 1-21.

Kanamori, H. (1977). The energy release in great earthquakes. *Journal of Geophysical Research*, 82, 20, pp. 2981-2987.

Mansinha, L., & Smylie, D.E., (1971). The displacement field of inclined faults. *Bulletin of the Seismological Society of America,* 61, 5, pp. 1433–1440.

Mokhtari, M., Abdollahie, I., & Khaled Hessami, H. (2008). Structural elements of the Makran region, Oman sea and their potential relevance to tsunamigenisis. *Natural Hazards*, 47, pp. 185–199.

Heidarzadeh, M., Pirooz, M.D., Zaker, N.H., Yalciner, A.C., Mokhtari, M., & Esmaeily, A. (2008). Historical tsunami in the Makran subduction zone off the southern coasts of Iran and Pakistan and results of numerical modeling. *Ocean Engineering* 35, 8 & 9, pp. 774–786.

Hidayat, D. ; Barker, J.S., & Satake, K. (1995). Modeling the seismic source and tsunami generation of the December 12, 1992 Flores Island, Indonesia, earthquake. *Pure and Applied Geophysics,* 144, 3 &4, pp. 537-554.

IOC, IHO, & BODC (2003), Centenary edition of the GEBCO digital atlas, published on CD-ROM on behalf of the Intergovernmental Oceanographic Commission and the International Hydrographic Organization as part of the general bathymetric chart of the oceans, British oceanographic data centre, Liverpool.

Okal, E.A., & Synolakis, C.E. (2008). Far–field tsunami hazard from mega–thrust earthquakes in the Indian Ocean. *Geophysical Journal International* , 172, 3, pp. 995–1015.

Page, W.D., Alt, J.N., Cluff, L.S., Plafker, G. (1979). Evidence for the recurrence of large–magnitude earthquakes along the Makran coast of Iran and Pakistan. *Tectonophysics*, 52, pp. 533–547.

Park, J.-O., Tsuru, T., Kodaira, S., Cummins, Ph.R., & Kaneda,Y. (2002). Splay fault branching along the Nankai subduction zone, Science, 297, pp. 1157-1160.

Poliakov, A.N.B., Dmowska, R., & Rice, J.R. (2002). Dynamic shear rupture interactions with fault bends and off-axis secondary faulting, *Journal of Geophysical Research,* 107, B11, pp. 1-18.

Plafker, G. (1972). Alaskan earthquake of 1964 and Chilean earthquake of 1960: implications for arc tectonics. *Journal of Geophysical Research,* 77, pp. 901–923.

Plafker, G., Ward, S.N., Nishenko, S.P., Cluff, L.S., Coonrad, J., & Syahrial, D. (2007). Evidence for a secondary tectonic source for the cataclysmic tsunami of 12/26/2004 on NW Sumatra. *Seismological Society of America*, Annual meeting, Kona, Hawaii, April 11–13. Abstract.

Quittmeyer, R.C., & Jacob, K.H. (1979). Historical and modem seismicity of Pakistan, Afghanistan, northwestern India, and southeastern Iran. *Bulletin of the Seismological Society of America*, 69, 3, pp. 773–823.

Ryan, H.F., & Scholl, D.W. (1989). The evolution of forearc structures along an oblique convergent margin, central Aleutian Arc. *Tectonics*, 8, pp. 497–516.

Schulson, E.M., Iliescu, D., & Renshaw, C.E. (1999). On the initiation of shear faults during brittle compressive Failure: A new mechanism, *Journal of Geophysical Research,* 104, B1, pp. 695-705.

Sibuet, J.C., et al. (2007). 26th December 2004 great Sumatra–Andaman earthquake: Co–seismic and post–seismic motions in northern Sumatra. *Earth and Planetary Science Letters,* 263, pp. 88–103.

Stein, S., Okal, E.A. (2007). Ultralong period seismic study of the December 2004 Indian Ocean earthquake and implications for regional tectonics and the subduction process. *Bulletin of the Seismological Society of America*, 97, 1A, pp. S279–S295.

Sykes, L.R., & Menke, W. (2006). Repeat times of large earthquakes: implications for earthquake mechanics, *Bulletin of the Seismological Society of America,* 96, 5, pp. 1569–1596.

Sunagawa, Y., & Hayashi, D. (2007). Development of splay faults in the Nankai Accretionary prism, *Bull. Fac. Sci.,Univ. Ryukyus*, 84 , pp. 15 -31.

Synolakis, C.E. (2003). Tsunami and seiche. In: *Earthquake Engineering Handbook*, CRC Press, W. F Chen., & C. Scawthorn (Eds.), Chapter 9, pp. 1–90.

Synolakis, C.E. ; & Okal, E.A. (2005). 1992-2002: Perspective on a decade of post-tsunami surveys, in: Tsunami ed. by K. Satake, *Advances in Natural and Technological Hazards*, 23, pp. 1–30.

Tinti, S., Armigliato, A., Manucci, A., Pagnoni, G., Zaniboni, F., Yalciner, A.C., and Altinok, Y. (2006). The generating mechanisms of the August 17, 1999 Izmit Bay (Turkey) tsunami: Regional (tectonic) and local (mass instabilities) causes. *Marine Geology*, 225, pp. 311–330.

Titov, V.V., and Synolakis, C.E. (1997). Extreme inundation flow during the Hokkaido-Nansei-Oki tsunami. *Geophysical Research Letters,* 24, pp. 1315–1318.

Wang, K., & Hu., Y. (2006). Accretionary prisms in subduction earthquake cycles: The theory of dynamic Coulomb wedge, *Journal of Geophysical Research*, 111, B06410, pp. 1-16.

Wells, D.L., & Coppersmith, K.J. (1994). New empirical relationships among magnitude, rupture length, rupture width, rupture area, and surface displacement. *Bulletin of the Seismological Society of America*, 84, 4, pp. 974–1002.

Yalciner, A.C., Pelinovsky, E., Talipova, T., Kurkin, A., Kozelkov, A., and Zaitsev, A. (2004). Tsunamis in the Black Sea: comparison of the historical, instrumental, and numerical data. *Journal of Geophysical Research,* 109, 12, pp. 2003–2113.

Yeh, H., Liu, P., & Synolakis, C.E. (1996). Long wave runup models. World Scientific Publication Company, London, 403 pp.

The Tsunami Threat - Research and Technology

Edited by Nils-Axel MÃ¶rner

ISBN 978-953-307-552-5
Hard cover, 714 pages
Publisher InTech
Published online 29, January, 2011
Published in print edition January, 2011

Submarine earthquakes, submarine slides and impacts may set large water volumes in motion characterized by very long wavelengths and a very high speed of lateral displacement, when reaching shallower water the wave breaks in over land - often with disastrous effects. This natural phenomenon is known as a tsunami event. By December 26, 2004, an event in the Indian Ocean, this word suddenly became known to the public. The effects were indeed disastrous and 227,898 people were killed. Tsunami events are a natural part of the Earth's geophysical system. There have been numerous events in the past and they will continue to be a threat to humanity; even more so today, when the coastal zone is occupied by so much more human activity and many more people. Therefore, tsunamis pose a very serious threat to humanity. The only way for us to face this threat is by increased knowledge so that we can meet future events by efficient warning systems and aid organizations. This book offers extensive and new information on tsunamis; their origin, history, effects, monitoring, hazards assessment and proposed handling with respect to precaution. Only through knowledge do we know how to behave in a wise manner. This book should be a well of tsunami knowledge for a long time, we hope.

INTECH
open science | open minds

InTech Europe
University Campus STeP Ri
Slavka Krautzeka 83/A
51000 Rijeka, Croatia
Phone: +385 (51) 770 447
Fax: +385 (51) 686 166
www.intechopen.com

InTech China
Unit 405, Office Block, Hotel Equatorial Shanghai
No.65, Yan An Road (West), Shanghai, 200040, China
中国上海市延安西路65号上海国际贵都大饭店办公楼405单元
Phone: +86-21-62489820
Fax: +86-21-62489821

IntechOpen